Quantifying the yield stress of bentonite muds mixed with other clays during drilling operations

Alexis Bougouin, A. Pantet, N.-D. Ahfir

Quantifying the yield stress of bentonite muds mixed with other clays during drilling operations

A. Bougouin*

Aix-Marseille Université, CNRS, IUSTI, Marseille, France

A. Pantet*, N.-D. Ahfir

Laboratoire Ondes et Milieux Complexes (LOMC) - Université Le Havre Normandie, UMR 6294 CNRS, 76063 Le Havre, France

Abstract

In civil engineering, bentonite-water mixtures, commonly referred to as drilling muds, are intensively used in order to lubricate tools, consolidate walls, and help extracting cuttings during drilling operations. The efficiency of drilling muds in each of these tasks lies in their rheological properties depending mainly on the amount of clay materials. During the field works, drilling muds are mixed with the excavated soil materials (e.g., sand, clay, organic matter) that may change drastically the rheological properties of mixtures. With the aim of understanding better the rheology of field drilling muds mixed with other clays, rheological measurements on mono- and binary-clay suspensions were performed using a rotational rheometer equipped with coaxial cylinders, for which the type of clay materials (i.e., bentonite, kaolin and illite), the total clay volume fraction φ_t and the bentonite to clay volume ratio R_b were varied. The contribution of this work is twofold: (i) to highlight the major role of φ_t and R_b independently on the rheology of binary-clay suspensions and (ii) to provide phenomenological models to quantify the dependency of the yield stress on both φ_t and R_b that would be particularly useful for industrial applications.

Keywords: Binary suspension, Clay, Drilling mud, Rheology, Yield stress

*Corresponding author

Email addresses: alexis.bougouin@univ-amu.fr (A. Bougouin), anne.pantet@univ-lehavre.fr (A. Pantet)

Accepted in Applied Clay Science

1. Introduction

In the field of civil engineering, drilling muds or slurries, usually composed of bentonite, water and additives (like polymers) are intensively used for underground works with the aim of lubricating tools, consolidating walls thanks to the hydrostatic pressure and the cake formation and helping to extract cuttings during the excavation works. The efficiency of drilling muds is mainly related to their rheological properties depending on many parameters, such as the amount of bentonite (Choo and Bai, 2015), the pH (Brenna et al., 1999; Kelessidis et al., 2007; Choo and Bai, 2015; Gamal et al., 2019), the temperature (Mohammed, 2017), and the type of additives used (Vipulanandan and Mohammed, 2014; Du et al., 2020; Abu-Jdayil et al., 2021). Among them, the amount of bentonite within the drilling muds, commonly referred to as the volume fraction, the mass fraction or the bulk density, is one of major control parameters affecting the rheological properties, especially the apparent viscosity and the yield stress (i.e., the minimum stress to flow) of suspensions.

With the aim of predicting the yield stress of mono-clay suspensions (i.e., composed of one-clay material), several phenomenological models were proposed depending on the clay volume fraction φ_t with fitting parameters allowing to take into account the intrinsic properties of clay materials used (O'Brien and Julien, 1988; Zhou et al., 1999; Flatt and Bowen, 2006; Spearman, 2017). Recently, it was shown that the model type of Zhou et al. (1999) and Spearman (2017) was the most appropriate one to predict the yield stress of non-thixotropic clay suspensions over a wide range of clay volume fractions (Bougouin et al., 2022). This model reads as

$$\widehat{\tau}_y(\varphi_t) = \alpha \left(\frac{\varphi_t}{\varphi_m - \varphi_t} \right)^{\beta}, \tag{1}$$

where α and β are two fitting parameters, and φ_m is the maximum volume fraction at which the yield stress should diverge. Note that this latter one can be found equal to $\varphi_m = 1$ (Zhou et al., 1999) or $\varphi_m = 0.64$ (Spearman, 2017) based on the idea that the maximum volume fraction is equal to the volume fraction of clay sheets on top of the other (i.e., like a package of papers) or the random close packing of spherical, solid and monodisperse clay stacks, respectively. These two values of φ_m are questionable, but it remains a difficult challenge to investigate hyperconcentrated clay suspensions at the laboratory scale.

The rheological behaviour of bentonite suspensions strongly differs from that of suspensions made of other clay materials (e.g., kaolin, illite). Bentonite-

water mixtures are usually characterized by thixotropic effects (i.e., time-dependent shear stress) and significantly higher shear stresses under similar conditions, which is attributed to the type of clay minerals contained inside. Two different properties are usually used to classify clay minerals, namely the swelling behaviour (expanding mineral or not) and the basic crystallographic repeat unit (octahedral/tetrahedral sheets - noted as O and T, respectively, in the following) of the layer structure. Overall, the layer structure of clay minerals is splitted into TO (1:1) - 7Å (kaolinite), TOT (2:1) - 10-20Å (illite, smectite) and TOT:O (2:1:1) - 14Å (chlorite), while only the TOT (2:1) - 10-20Å category is subdivided upon its swelling property (Chassagne, 2021). In fact, only the low mineral charge of smectites allows hydrated ions to be inserted between the clay mineral layers conferring them a swelling property, and thus a peculiar behaviour of bentonite suspensions mainly composed of montmorillonite (a part of smectites) and other minority minerals (e.g., quartz, mica, oxides, zeolites).

During the excavation operations, bentonite drilling muds are mixed with the excavated soil materials (e.g., sand, clay, organic matter) that may affect drastically the rheological properties of suspensions. In particular, different types of clay soils may be encountered depending on the geological context and the early or intermediate stages of weathering. Then, bentonite drilling muds may be less efficient than as expected, requiring to anticipate such modifications with the type and the amount of excavated soil materials. The addition of sand within mono-clay suspensions, and more generally, that of coarse grains within yield stress fluids, has already been intensively studied through laboratory experiments and theoretical models (Ancey and Jorrot, 2001; Mahaut et al., 2008a,b; Chateau et al., 2008; Pantet et al., 2010; Ovarlez et al., 2015; Hafid et al., 2016; Pellegrino and Schippa, 2018; Nguyen et al., 2018; Vu et al., 2018; Bougouin et al., 2022). Overall, the presence of coarse grains contributes to increase viscous dissipation in the system promoting larger apparent viscosities, larger yield stresses and larger elastic modulus of suspensions. From a purely mechanical point of view, Chateau et al. (2008) proposed predictive models to estimate the dependency of the rheological parameters of suspensions on the coarse volume fraction based on a nonlinear homogenization approach. In the field, however, the contribution of coarse grains can be significantly reduced by desanding recycled and re-used drilling muds, which is a more complex process with clayey cuttings. In the case of binary-clay suspensions (i.e., composed of two-clay materials), both the total of clay content and the relative proportion of clay materials modify the rheological behaviour of suspensions (Neaman and Singer, 2000; Chemeda et al., 2014; Shakeel et al., 2021a). In

contrast to coarse-grained clay suspensions, however, no predictive models exist to quantify the relative influence of these two parameters on their rheological properties, and more particularly on their yield stress.

In this general context, the present study addressed the rheological behaviour of binary-clay suspensions with the aim of helping the modelling of drilling muds mixed with other clays for the excavation operation success. More specifically, rheological measurements of bentonite-kaolin and bentonite-illite suspensions were performed using a rheometer equipped with a coaxial cylinders, for which both the total clay volume fraction and the bentonite to clay volume ratio were varied independently.

2. Rheometer device and clay materials

Rheological measurements of clay suspensions were performed using an Anton Paar RheolabQC rheometer equipped with coaxial cylinders (outer radius: $R_o = 14.5$ mm; inner radius: $R_i = 13.4$ mm; height of the inner cylinder: $h = 40.0$ mm). The rheological procedure of measurements was defined as follows. First, a pre-shearing was applied to the suspension at 100 s^{-1}, for 30 seconds. Then, it was left at rest to obtain a structural reference state, for 120 seconds. Finally, the suspension was sheared by increasing and then decreasing the shear rate $\dot{\gamma}$ logarithmically between 1 s^{-1} and 10^3 s^{-1}, referred to as up and down logarithmic ramps, respectively, in the following. Note that other measurement protocols drawn from Shakeel et al. (2021b), were considered without changing the following results. Moreover, some specific cautions were taken to avoid a misinterpretation of results. In order to anticipate a viscous-to-inertial transition within the suspensions, the Taylor number was estimated as

$$T_a = 2\pi N \frac{\rho_s R_i (R_o - R_i)}{\eta_s} \left(\frac{R_o - R_i}{R_o} \right)^{1/2}, \tag{2}$$

where N is the rotational speed (in rev.s^{-1}), R_o and R_i are the outer and inner radius of coaxial cylinders, respectively, and ρ_s and η_s are the bulk density and the apparent viscosity of suspensions, respectively. According to Matignon et al. (2014), the rheological measurements satisfying $Ta \geq 40$ were disregarded because of inertial effects within the suspension. Moreover, at low shear rate, any measurement that deviated surprisingly from the expected trend (e.g., abrupt change in slope, decrease of the shear stress with increasing shear rate) was also ignored attributed to experimental artefacts, such as wall slip (Meeker et al., 2004; Ballesta et al., 2012) and shear

banding (Ovarlez et al., 2009; Kaci et al., 2009; Schall and Van Hecke, 2010; Ovarlez et al., 2013).

Suspensions were made of tap water mixed with one or two types of clay materials, referred to as mono- and binary-clay suspensions, respectively, in the following. Tap water was characterized by a pH of 7.5 ± 0.1, an electrical conductivity of 0.58 ± 0.05 mS.cm^{-1}, an hardness of 24 ± 2 mg/l as $CaCO_3$ and an alcalinity of 20 ± 2 mg/l as $CaCO_3$. The types of clay materials used were bentonite (bentonite 1 - 35% calcite, 33% montmorillonite, 32% quartz; bentonite 2 - montmorillonite, interstratified illite-montmorillonite, kaolinite, halloysite; bentonite 3 - montmorillonite, interstratified illite-montmorillonite, kaolinite, halloysite), kaolin (kaolin 1 - 67% kaolinite, 17% quartz, 16% illite; kaolin 2 - 56% kaolinite, 38% biotite, 6% quartz) and illite (47% illite, 47% calcite, 6% quartz), corresponding to mineral mixtures with a high content of montmorillonite, kaolinite and illite, respectively. The term 'illite' is commonly used to define both mineral and clay material, and it would be referred only to the clay material in the following. Recall that X-ray diffraction (XRD) provides only a semi-quantification of the mineralogical composition of clay materials, and these measurements allowed only to identify major minerals within the clay materials used. On the other hand, bentonites 2 and 3 corresponded to industrial samples and they had probably undergone specific treatments. For this reason, the determination of the crystallographic structure was much more complex with a standard analysis from X-ray diffraction, and the mass proportion of minerals was therefore not provided here. The particle size of each clay material was measured with a Malvern Mastersizer 2000 analyser, and it was found as $d_b = 34^{+125}_{-30}$ μm (bentonite 1), $d_b = 28^{+75}_{-16}$ μm (bentonite 2), $d_b = 52^{+96}_{-28}$ μm (bentonite 3), $d_k = 7^{+16}_{-5}$ μm (kaolin 1), $d_k = 11^{+208}_{-9}$ μm (kaolin 2), and $d_i = 4^{+10}_{-3}$ μm (illite), where the given values corresponds to the size of clay stacks for which 10%, 50%, and 90% of the total volume of particles is below. The particle densities of bentonite, kaolinite and illite were estimated as $\rho_b = 2650$ kg.m^{-3}, $\rho_k = 2550$ kg.m^{-3} and $\rho_i = 2500$ kg.m^{-3}, respectively, from direct measurements (Bougouin et al., 2022) and values given in the literature (Coussot, 1997).

The preparation of suspensions required several specific stages. First, each type of clay materials was weighed and mixed manually with water. Then, the suspensions were left at rest at least one day before the rheological measurements to ensure a proper hydration of clay materials. In presence of bentonite materials, a second step of mixing was carried out with a propeller for 5 minutes after a dozen hours of hydratation to eliminate sustainable

aggregates. Finally, the suspensions were remixed manually for 10 minutes before to set up within the cup of the rheometer. Note that the pH of suspensions was found to be roughly constant in the range $9 - 10$. To characterize the suspensions, both the total clay volume fraction φ_t and the bentonite to clay volume ratio R_b were defined as

$$\varphi_t = \frac{(\rho_{k/i} m_b + \rho_b m_{k/i})\rho_w}{\rho_{k/i}\rho_w m_b + \rho_b \rho_w m_{k/i} + \rho_b \rho_{k/i} m_w}, \tag{3}$$

$$R_b = \frac{\rho_{k/i} m_b}{\rho_{k/i} m_b + \rho_b m_{k/i}}, \tag{4}$$

where m_b, $m_{k/i}$ and m_w are the masses of bentonite, kaolin or illite and water, respectively, and $\rho_w = 1000\ \mathrm{kg.m^{-3}}$ is the water density. In the present study, both the total volume fraction φ_t and the bentonite to clay volume ratio R_b were varied over a wide range summarized in Table 1.

Table 1: Summary table of mono- and binary-clay suspensions with the type of clay materials used, the total clay volume fraction φ_t (Eq. 3) and the bentonite to clay volume ratio R_b (Eq. 4).

		Type of clay materials	Total clay volume fraction φ_t [-]	Bentonite to clay volume ratio R_b [-]
Mono-clay	suspensions	Bentonite 1	[0.03 : 0.097]	1
		Bentonite 2	[0.015 : 0.099]	1
		Bentonite 3	[0.016 : 0.08]	1
		Kaolin 1	[0.052 : 0.301]	0
		Kaolin 2	[0.1 : 0.301]	0
		Illite	[0.1 : 0.302]	0
Binary-clay	suspensions	Bentonite 1 Kaolin 1	0.06 [0.05 : 0.15] [0.091 : 0.292]	[0.3 : 0.9] 0.5 [0.13 : 0.61]
		Bentonite 1 Kaolin 2	[0.061 : 0.15]	[0.31 : 0.9]
		Bentonite 1 Illite	[0.06 : 0.248]	[0.19 : 0.8]
		Bentonite 2 Kaolin 1	[0.066 : 0.17]	[0.15 : 0.74]
		Bentonite 3 Kaolin 1	[0.063 : 0.159]	[0.1 : 0.95]

3. Rheological results

3.1. Mono-clay suspensions: bentonite vs. kaolin/illite

The rheological behaviour of mono-clay suspensions, i.e. composed of one-clay material, was first addressed to quantify the influence of both the type and the total volume fraction φ_t. Hence, the bentonite to clay volume ratio R_b was reduced to 0 and 1 for kaolin or illite and bentonite suspensions, respectively (see Table 1).

Figure 1 shows the shear stress τ (inset : the apparent viscosity η_s) as a function of the shear rate $\dot{\gamma}$ for (a) bentonite suspensions and (b) kaolin suspensions with increasing the total clay volume fraction φ_t. Regardless of the type and the volume fraction of clay materials, the rheology of suspensions was characterized by a yielding and shear-thinning behaviour successfully described by the Herschel-Bulkley model (lines), as expected for mono-clay suspensions (Coussot and Piau, 1994). Quantitatively, the rheological properties of suspensions were strongly dependent on both the type and the volume fraction φ_t of clay materials. In particular, at lower φ_t and at a given $\dot{\gamma}$, bentonite suspensions exhibited much larger values of shear stresses τ and apparent viscosities η_s compared to kaolin suspensions. The same conclusions were also drawn between bentonite and illite suspensions (not shown here). This was attributed to the higher level of cohesiveness of the montmorillonite-containing bentonite materials in comparison with kaolin and illite. Moreover, the increase of the total clay volume fraction φ_t also promoted larger shear stresses τ and apparent viscosities η_s, for a given type of clay materials. The addition of clay materials within the suspension reduced the mean distance between clay stacks strengthening cohesion and increasing viscous dissipation by decreasing the size of interstices, in which water was sheared. Finally, one observed that the flow curves of bentonite suspensions mismatched between up (upward triangles) and down (downward triangles) logarithmic ramps, which was hardly reported for kaolin and illite suspensions. Such an observation of lower down flow curves than up ones was the sign of thixotropic effects attributed to a longer timescale to reach the microstructural steady-state compared to the time of measurements (Paumier, 2007). Although thixotropy is an important property of bentonite suspensions, the associated variations on the yield stress studied in the following, were much lower than those due to the type and the wide range of volumes fractions of clay materials considered (see Supplementary Material, available online). Thus, thixotropic effects of suspensions containing bentonite were disregarded in the following. In the same way, it could be mentioned that, for kaolin and illite suspensions, up flow curves were

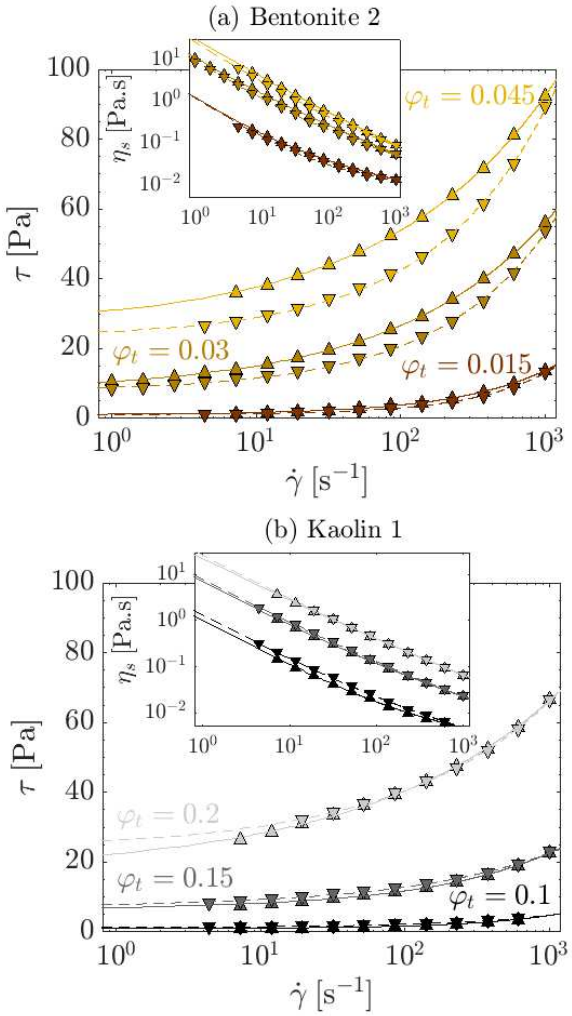

Figure 1: Shear stress τ (inset: apparent viscosity η_s) as a function of the shear rate $\dot{\gamma}$ during up (upward triangles and solid lines) and down (downward triangles and dashed lines) logarithmic ramps, for mono-clay suspensions with various φ_t. Lines correspond to the best fit of the Herschel-Bulkley model $\tau = \tau_y + K\dot{\gamma}^n$ (inset: $\eta_s = \tau_y/\dot{\gamma} + K\dot{\gamma}^{n-1}$), with the yield stress τ_y, the consistency K and the flow index n.

slightly lower than down flow curves probably due to a modification of the internal structure of suspensions. In any case, the variations between up and down flow curves were considered by adding error bars in the following when larger than the size of symbols.

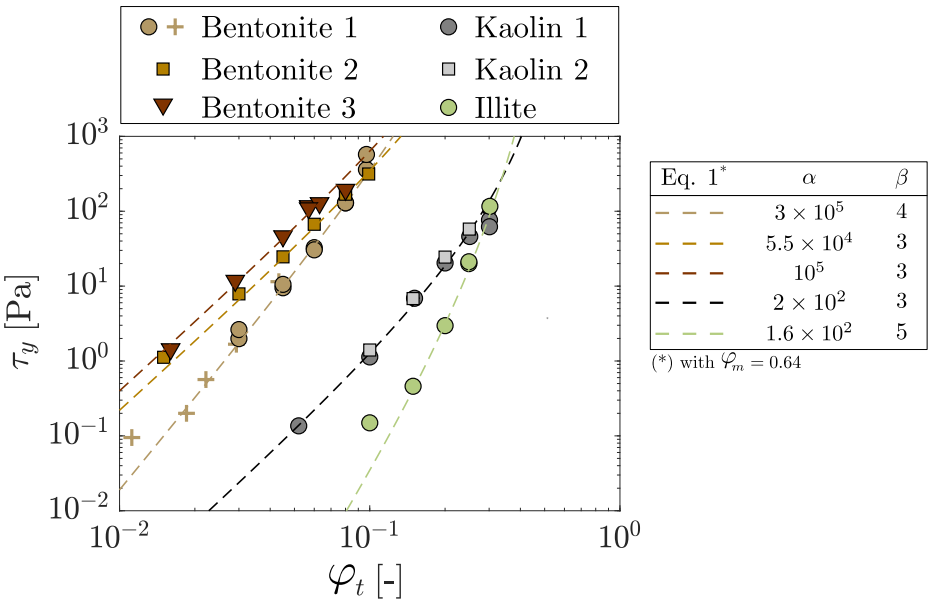

Figure 2: Yield stress τ_y of mono-clay suspensions as a function of the total clay volume fraction φ_t. (- - -) Spearman's model (Eq. 1, with $\varphi_m = 0.64$). Crosses correspond to additional experiments of suspensions made of bentonite 1 using other procedures of preparation and measurement than defined in Sec. 2.

The yield stress τ_y is one of the main physical properties of clay suspensions and it could be easily extracted from the best fit of the Herschel-Bulkley model. In Fig. 2, the yield stress τ_y of mono-clay suspensions was shown as a function of the total clay volume fraction φ_t, for each type of clay materials used. Firstly, one clearly observed that the yield stress τ_y of bentonite suspensions was much larger than that of kaolin and illite suspensions, at a given φ_t. As discussed above, it was attributed to the high level of cohesiveness of montmorillonite-containing bentonite materials in comparison with the other types of clay materials, i.e. kaolin and illite. Moreover, the yield stress τ_y was strongly dependent on the total clay volume fraction φ_t, which was well predicted by the Spearman's model (Eq. 1, with $\varphi_m = 0.64$) as shown by the dashed lines. The relevance of this model quantifying the φ_t-dependency of the yield stress has already been reported for kaolin and illite suspensions over a wide range of volume fractions (Bougouin et al., 2022), while it was shown here to be also appropriate in the case of bentonite suspensions. The two fitting parameters (α, β) were dependent on the type of

clay materials used, and thus directly related to their intrinsic properties. Here, it was found that the prefactor α was in the order of magnitude of 10^2 and $10^4 - 10^5$ for kaolin/illite and bentonite materials, respectively, while the exponent β was included in the range $[3:5]$. Although different batches of bentonite were used, the specific behaviour of the major clay mineral (i.e., montmorillonite) contained inside allowed to distinguish clearly bentonite suspensions from others. Nevertheless, the variability of the couple (α, β) in the case of bentonite suspensions suggested that other parameters, such as the presence of other minority minerals and additives, powder quality or activation process, should also be considered to predict totally the yield stress of suspensions.

3.2. Binary-clay suspensions: bentonite-kaolin and bentonite-illite

The rheological behaviour of binary-clay suspensions made of bentonite and another type of clay materials, namely kaolin or illite, was then addressed by varying both the total clay volume fraction φ_t and the bentonite to clay volume ratio R_b independently.

In this way, Fig. 3 shows the shear stress τ (inset: the apparent viscosity η_s) as a function of the shear rate $\dot{\gamma}$ during up and down logarithmic ramps, at (a) constant $R_b = 0.5$ and φ_t varied and (b) constant $\varphi_t = 0.06$ and R_b varied. As expected, the increase of the total clay volume fraction φ_t promoted larger shear stresses τ and larger apparent viscosities η_s, as already discussed for mono-clay suspensions. Additionally, at constant φ_t, the bentonite to clay volume ratio R_b also affected significantly the rheological behaviour of suspensions due to different properties of clay minerals contained in bentonite and kaolin/illite. Thus, both parameters should be considered to fully describe the rheological properties, and in particular the yield stress, of binary-clay suspensions.

Beyond this idea, a phenomenological model taking into account the dependency of the yield stress τ_y of binary-clay suspensions on both the total clay volume fraction φ_t and the bentonite to clay volume ratio R_b was developed. First, it was argued that the yield stress of binary-clay suspensions was bounded by the upper yield stress $\tau_y(\varphi_t, R_b = 1) = \tau_y^b$ of mono-clay suspensions made of bentonite and the lower yield stress $\tau_y(\varphi_t, R_b = 0) = \tau_y^{k/i}$ of mono-clay suspensions made of kaolin or illite (more details given in Supplementary Material, available online). Moreover, both quantities τ_y^b and $\tau_y^{k/i}$ could be well predicted by the Spearman's model (Eq. 1, with $\varphi_m = 0.64$) as shown in Sec. 3.1, referred to as $\widehat{\tau}_y^b$ and $\widehat{\tau}_y^{k/i}$ for bentonite and kaolin/illite suspensions, respectively, in the following. Finally, the

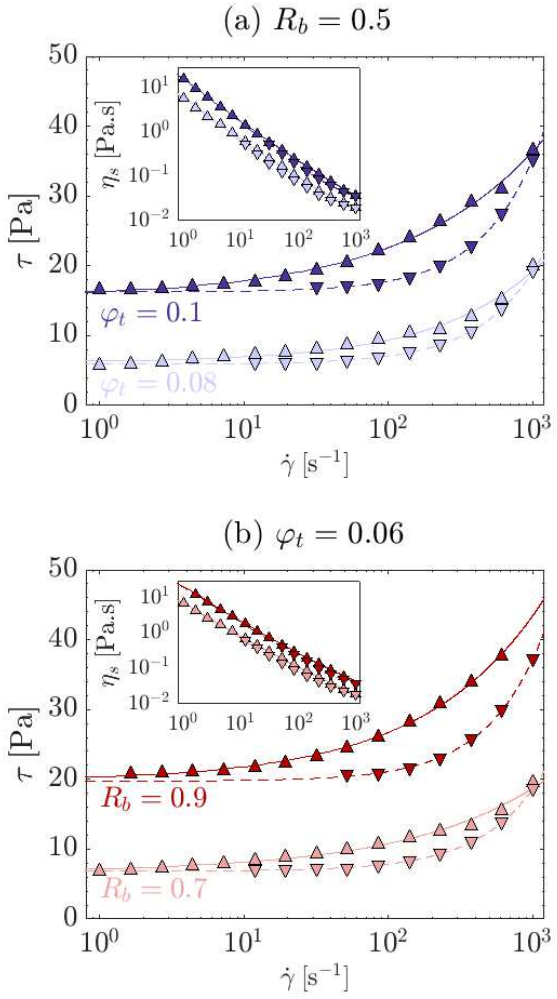

Figure 3: Shear stress τ (inset: apparent viscosity η_s) as a function of the shear rate $\dot{\gamma}$ during up (upward triangles and solid lines) and down (downward triangles and dashed lines) logarithmic ramps, for binary-clay (bentonite 1 - kaolin 1) suspensions at (a) constant $R_b = 0.5$ and $\varphi_t = [0.08, 0.1]$ and (b) constant $\varphi_t = 0.06$ and $R_b = [0.7, 0.9]$. Lines correspond to the best fits of the Herschel-Bulkley model $\tau = \tau_y + K\dot{\gamma}^n$ (inset : $\eta = \tau_y/\dot{\gamma} + K\dot{\gamma}^{n-1}$), with the yield stress τ_y, the consistency K, and the flow index n.

trend of the yield stress τ_y with R_b could be addressed through the quantity $(\tau_y - \widehat{\tau}_y^{k/i})/(\widehat{\tau}_y^{b} - \widehat{\tau}_y^{k/i})$ bounded between 0 and 1 when $R_b = 0$ and 1, respectively.

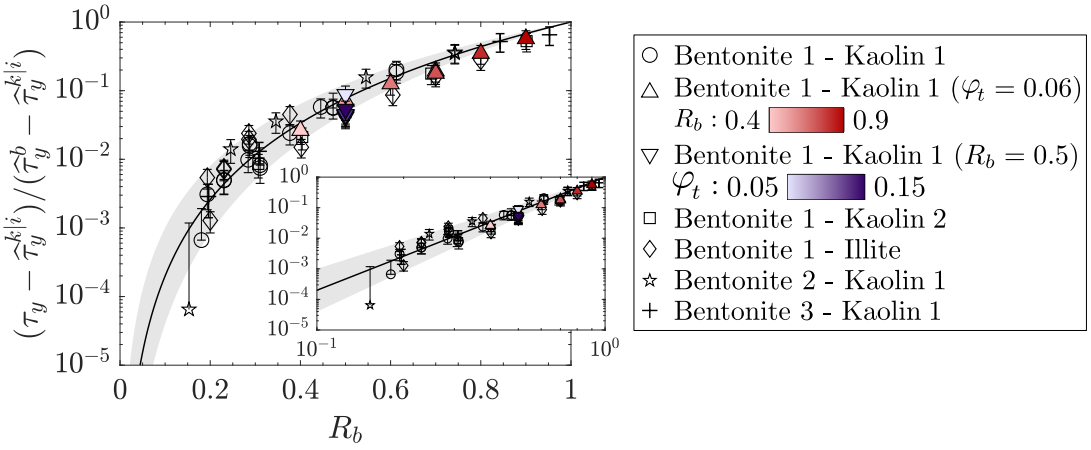

Figure 4: Quantity $(\tau_y - \widehat{\tau}_y^{k/i})/(\widehat{\tau}_y^{b} - \widehat{\tau}_y^{k/i})$ as a function of the bentonite to clay volume ratio R_b for the whole set of binary-clay suspensions, where $\widehat{\tau}_y^{k/i}$ and $\widehat{\tau}_y^{b}$ are the yield stresses of mono-clay suspensions made of kaolin/illite and bentonite, respectively, estimated by the Spearman's model (Eq. 1, with $\varphi_m = 0.64$) as fitted in Fig. 2. The solid line and gray area correspond to $(\tau_y - \widehat{\tau}_y^{k/i})/(\widehat{\tau}_y^{b} - \widehat{\tau}_y^{k/i}) = R_b^{\lambda}$ with $\lambda = 3.7 \pm 0.7$.

Figure 4 shows the quantity $(\tau_y - \widehat{\tau}_y^{k/i})/(\widehat{\tau}_y^{b} - \widehat{\tau}_y^{k/i})$ as a function of the bentonite to clay volume ratio R_b for the whole set of binary-clay suspensions considered in this study. Overall, the quantity $(\tau_y - \widehat{\tau}_y^{k/i})/(\widehat{\tau}_y^{b} - \widehat{\tau}_y^{k/i})$ increased with increasing the values of R_b until reaching a value of 1, as expected. Moreover, the trend of $(\tau_y - \widehat{\tau}_y^{k/i})/(\widehat{\tau}_y^{b} - \widehat{\tau}_y^{k/i})$ with R_b was broadly independent on the type and the total volume φ_t of clay materials. To confirm such an observation, downward and upward triangles correspond to the trend of $(\tau_y - \widehat{\tau}_y^{k/i})/(\widehat{\tau}_y^{b} - \widehat{\tau}_y^{k/i})$ at constant $R_b = 0.5$ and constant $\varphi_t = 0.06$ with increasing φ_t and R_b, respectively. This means that, at least at first order, the yield stress of binary-clay suspensions was mainly controlled by the type and the amount of clay materials contained inside, without physicochemical interactions between different minerals. More quantitatively, one obtained a master curve given by $(\tau_y - \widehat{\tau}_y^{k/i})/(\widehat{\tau}_y^{b} - \widehat{\tau}_y^{k/i}) = R_b^{\lambda}$ with $\lambda = 3.7 \pm 0.7$ (solid line and gray area). To conclude on, the yield stress of binary-clay suspensions may thus be quantified by the relation

$$\tau_y(\varphi_t, R_b) = R_b^{\lambda}\widehat{\tau}_y^{b}(\varphi_t) + (1 - R_b^{\lambda})\widehat{\tau}_y^{k/i}(\varphi_t), \tag{5}$$

where $\widehat{\tau}_y^{b}$ and $\widehat{\tau}_y^{k/i}$ are the yield stresses of mono-clay suspensions made of bentonite and kaolin/illite, respectively, estimated by the Spearman's

model (Eq. 1, with $\varphi_m = 0.64$), and $\lambda = 3.7 \pm 0.7$ is an empirical constant parameter. Note that, for $R_b < 0.2$, the accuracy of measurements could lead to negative values of $(\tau_y - \widehat{\tau}_y^{k/i})/(\widehat{\tau}_y^{b} - \widehat{\tau}_y^{k/i})$, i.e. $\tau_y < \widehat{\tau}_y^{k/i}$, and they were therefore disregarded.

To go further on, such an approach could be envisaged for predicting the yield stress of mono-clay suspensions by considering the rheology of mono-clay mineral suspensions, i.e. the rheology of suspensions made of each clay mineral contained in the clay material. However, some caution should be exercised because it will require to determine the rheological behaviour of each component contained in the clay material, while the present model was only established for two-component suspensions.

3.3. Towards the industrial applications

In the industrial field, the bulk density of drilling muds is usually preferred to the total clay volume fraction φ_t because of its ease of estimate in the fieldwork activities. Less rigorously, the previous models could then be expressed in this sense. In particular, both the total clay volume fraction φ_t and the bentonite to clay volume ratio R_b were substituted for the bulk density ρ_s and the density ratio $(\rho_s^* - \rho_w)/(\rho_s - \rho_w)$, where ρ_s^* is the bulk density of bentonite-water mixtures (i.e., without kaolin and illite), ρ_s is the bulk density of binary-clay suspensions, and ρ_w is the water density. Note that both ρ_s and $(\rho_s^* - \rho_w)/(\rho_s - \rho_w)$ were proportional to φ_t and R_b, respectively, because of the low variation in density of natural clay materials, i.e. $\rho_c \sim 2650 \pm 150\,\mathrm{kg.m^{-3}}$, and the low variation of the volume ratio $0.4 \lesssim (V_b + V_w)/(V_b + V_w + V_{k/i}) \leq 1$, with V_b, V_w, $V_{k/i}$ the volumes of bentonite, water and kaolin/illite, respectively. To finish with, both parameters ρ_s^* and ρ_s could be interpreted as the bulk densities of drilling muds before and after they were mixed with extruded clays.

Figure 5(a) shows first the increase of the yield stress τ_y with the bulk density ρ_s of mono-clay suspensions, as expected. The dependency of τ_y with ρ_s could be fairly well described by the ρ_s-dependent Spearman's model defined as

$$\widehat{\tau}_y(\rho_s) = \alpha \left(\frac{\rho_s - \rho_w}{\rho_m - \rho_s} \right)^{\beta}, \tag{6}$$

where α and β are two fitting parameters, and $\rho_m = \varphi_m \rho_c + (1 - \varphi_m)\rho_w = 2056\,\mathrm{kg.m^{-3}}$ (with $\varphi_m = 0.64$ and $\rho_c = 2650\,\mathrm{kg.m^{-3}}$) is the maximum bulk density. Note that the clay density ρ_c was kept constant here to maintain only two fittings parameters in Eq. 6, i.e. the couple (α, β), for the simplicity of industrial applications. This assumption led however to a slight increase

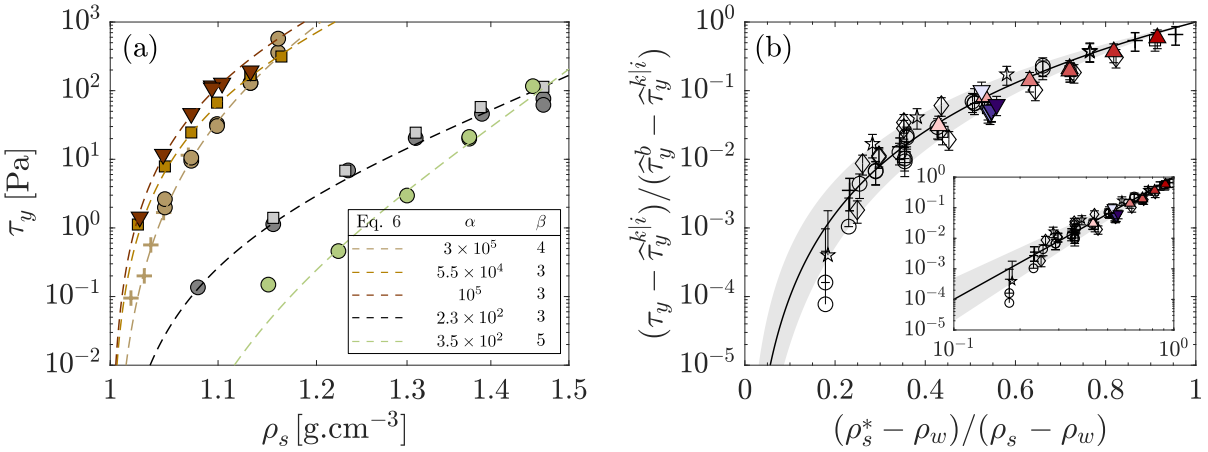

Figure 5: (a) Yield stress τ_y as a function of the bulk density ρ_s for the same set of mono-clay suspensions shown in Fig. 2. (- - -) ρ_s-dependent Spearman's model (Eq. 6). (b) Quantity $(\tau_y - \widehat{\tau}_y^{k/i})/(\widehat{\tau}_y^{b} - \widehat{\tau}_y^{k/i})$ as a function of the density ratio $(\rho_s^* - \rho_w)/(\rho_s - \rho_w)$ for the same set of binary-clay suspensions shown in Fig. 4. Here, ρ_s^* and ρ_s are the bulk densities of bentonite-water mixtures (i.e., without kaolin/illite) and binary-clay suspensions, respectively, ρ_w is the water density, and $\widehat{\tau}_y^{k/i}$ and $\widehat{\tau}_y^{b}$ are the yield stresses of mono-clay suspensions made of kaolin/illite and bentonite estimated by the ρ_s-dependent Spearman's model (Eq. 6), as fitted in Fig. 5(a). The solid line and gray area correspond to $(\tau_y - \widehat{\tau}_y^{k/i})/(\widehat{\tau}_y^{b} - \widehat{\tau}_y^{k/i}) = [(\rho_s^* - \rho_w)/(\rho_s - \rho_w)]^{\lambda}$ with $\lambda = 4.0 \pm 0.7$.

in values of α compared to those estimated in Fig. 2, for kaolin and illite suspensions.

Then, Fig. 5(b) shows the dependency of the quantity $(\tau_y - \widehat{\tau}_y^{k/i})/(\widehat{\tau}_y^{b} - \widehat{\tau}_y^{k/i})$ on the density ratio $(\rho_s^* - \rho_w)/(\rho_s - \rho_w)$ for the same set of binary-clay suspensions shown in Fig. 4. Here, the yield stresses $\widehat{\tau}_y^{k/i}$ and $\widehat{\tau}_y^{b}$ of mono-clay suspensions made of kaolin/illite and bentonite, respectively, were estimated by the ρ_s-dependent Spearman's model (Eq. 6). As previously concluded, data collapsed on a master curve independently on the type and the total volume fraction φ_t of clay materials. More specifically, it was found $(\tau_y - \widehat{\tau}_y^{k/i})/(\widehat{\tau}_y^{b} - \widehat{\tau}_y^{k/i}) = [(\rho_s^* - \rho_w)/(\rho_s - \rho_w)]^{\lambda}$ with $\lambda = 4.0 \pm 0.7$ (solid line and gray area) consistent with the value reported in the previous section. Thus, the yield stress of binary-clay suspensions could also be predicted less rigorously from the bulk density as

$$\tau_y(\rho_s, \rho_s^*) = \left(\frac{\rho_s^* - \rho_w}{\rho_s - \rho_w}\right)^{\lambda} \widehat{\tau}_y^{b}(\rho_s) + \left[1 - \left(\frac{\rho_s^* - \rho_w}{\rho_s - \rho_w}\right)^{\lambda}\right] \widehat{\tau}_y^{k/i}(\rho_s), \qquad (7)$$

where ρ_s^* and ρ_s are the bulk densities of bentonite-water mixtures (i.e., without kaolin/illite) and binary-clay suspensions, respectively, $\rho_w = 1000$ kg.m^{-3} is the water density, $\widehat{\tau}_y^{k/i}$ and $\widehat{\tau}_y^b$ are the yield stresses of mono-clay suspensions made of kaolinite/illite and bentonite, respectively, estimated by the ρ_s-dependent Spearman's model (Eq. 6), and $\lambda = 4.0 \pm 0.7$ is an empirical constant parameter.

Conclusion

In civil engineering, bentonite drilling muds are commonly used with the aim of lubricating tools, consolidating walls, and helping extracting cubblings for the drilling operation success. During the excavation works, bentonite drilling muds are progressively mixed with the excavated soil materials (e.g., sand, clay, organic matter) that may change drastically their rheological properties, and thus their efficiency in the achievement of their tasks. However, there is still a lack in predicting the modification of the rheology of drilling muds when they are mixed with other clays during drilling operations. In this objective, the rheological behaviour of mono- and binary-clay suspensions made of various types of clays materials (i.e., bentonite, kaolin, illite), was investigated using a rotational rheometer equipped with coaxial cylinders. Overall, the rheology of suspensions was characterized by a shear-thinning and yielding behaviour successfully described by the Herschel-Bulkley model $\tau = \tau_y + K\dot{\gamma}^n$, from which the yield stress τ_y, the consistency K and the flow index n could be deduced. More quantitatively, the rheological properties of suspensions were mainly controlled by the type of clay materials, the total clay volume fraction φ_t and the bentonite to clay volume ratio R_b. From the rheological measurements on mono-clay suspensions, it was first shown that the dependency of the yield stress τ_y on a wide range of the total clay volume fraction φ_t was fairly well described by the Spearman's model, for which the two fitting parameters were only dependent on the type of clay materials used. Then, the influence of both the total clay volume fraction φ_t and the bentonite to clay volume ratio R_b on the rheology of binary-clay suspensions was investigated independently. This approach allowed to propose a phenomenological model taking into account both φ_t and R_b for predicting the yield stress τ_y of binary-clay suspensions as $\tau_y(\varphi_t, R_b) = R_b^\lambda \widehat{\tau}_y^b(\varphi_t) + (1 - R_b^\lambda)\widehat{\tau}_y^{k/i}(\varphi_t)$, where $\widehat{\tau}_y^b$ and $\widehat{\tau}_y^{k/i}$ were the yield stresses of mono-clay suspensions made of bentonite and kaolin/illite previously estimated by the Spearman's model, respectively, and $\lambda = 3.7 \pm 0.7$ was an empirical constant parameter. Finally, the different predictive models were then expressed in light of the bulk density of suspensions usually

used in the industrial applications. These predictive models would be particularly useful for quantifying the yield stress of bentonite drilling muds mixed with other clays for the excavation operation success.

Acknowledgments

We are grateful to the Fédération Nationale des Travaux Publics and Soletanche Bachy, which have supported this work by funding internships. In particular, preliminary experiments were performed by Q. Ressouches during its internship. A. Bougouin was funded by the Normandy region with the project RIN SELINE. We thank B. Duchemin for conducting the analysis from X-ray diffraction (XRD).

References

Abu-Jdayil, B., Ghannam, M., Alsayyed Ahmed, K., Djama, M., 2021. The effect of biopolymer Chitosan on the rheology and stability of Na-bentonite drilling mud. Polymers 13, 3361.

Ancey, C., Jorrot, H., 2001. Yield stress for particle suspensions within a clay dispersion. J. Rheol. 45, 297–319.

Ballesta, P., Petekidis, G., Isa, L., Poon, W.C.K., Besseling, R., 2012. Wall slip and flow of concentrated hard-sphere colloidal suspensions. J. Rheol. 56, 1005–1037.

Bougouin, A., Benamar, A., Jarno, A., Marin, F., Pantet, A., 2022. Rheological behaviour of pure clay and coarse-grained clay suspensions using an inclined blade vane-in-cup. J. Non-Newton. Fluid Mech. 300, 104714.

Brenna, M., Kbir-Ariguib, N., Magnin, A., Bergaya, F., 1999. Effect of pH on rheological properties of purified Sodium bentonite suspensions. J. Colloid Interface Sci. 218, 442–455.

Chassagne, C., 2021. Introduction to colloid science: Applications to sediment characterization. TU Delft OPEN, Delft University of Technology, Delft, The Netherlands .

Chateau, X., Ovarlez, G., Trung, K.L., 2008. Homogenization approach to the behavior of suspensions of noncolloidal particles in yield stress fluids. J. Rheol. 52, 489–506.

Chemeda, Y.C., Christidis, G.E., Tauhid Khan, N.M., Koutsopoulou, E., Hatzistamou, V., Kelessidis, V.C., 2014. Rheological properties of palygorskite-bentonite and sepiolite-bentonite mixed clay suspensions. Appl. Clay Sci. 90, 165–174.

Choo, Y.K., Bai, K., 2015. Effects of bentonite concentration and solution pH on the rheological properties and long-term stabilities of bentonite suspensions. Appl. Clay Sci. 108, 182–190.

Coussot, P., 1997. Mudflow rheology and dynamics. Routledge, London .

Coussot, P., Piau, J.M., 1994. On the behavior of fine mud suspensions. Rheol. Acta 33, 175–184.

Du, M., Liu, P., Clode, P.L., Liu, J., Haq, B., Leong, Y.K., 2020. Impact of additives with opposing effects on the rheological properties of bentonite drilling mud: Flow, ageing, microstructure and preparation. J. Pet. Sci. Eng. 192, 107282.

Flatt, R.J., Bowen, P., 2006. A yield stress model for suspensions. J. Am. Ceram. Soc. 89, 1244–1256.

Gamal, H., Elkatatny, S., Basfar, S., Al-Majed, A., 2019. Effect of pH on rheological and filtration properties of water-based drilling fluid based on bentonite. Sustainability 11, 6714.

Hafid, H., Ovarlez, G., Toussaint, F., Jezequel, P.H., Roussel, N., 2016. Effect of particle morphological parameters on sand grains packing properties and rheology of model mortars. Cem. Concr. Res. 80, 44–51.

Kaci, A., Chaouche, M., Andreani, P.A., Brossas, H., 2009. Rheological behaviour of render mortars. Appl. Rheol. 19, 12794.

Kelessidis, V.C., Tsamantaki, C., Dalamarinis, P., 2007. Effect of pH and electrolyte on the rheology of aqueous Wyoming bentonite dispersions. Appl. Clay Sci. 38, 86–96.

Mahaut, F., Chateau, X., Coussot, P., Ovarlez, G., 2008a. Yield stress and elastic modulus of suspensions of noncolloidal particles in yield stress fluids. J. Rheol. 52, 287–313.

Mahaut, F., Mokeddem, S., Chateau, X., Roussel, N., Ovarlez, G., 2008b. Effect of coarse particle volume fraction on the yield stress and thixotropy of cementitious materials. Cem. Concr. Res. 38, 1276–1285.

Matignon, A., Ducept, F., Sieffermann, J.M., Barey, P., Desprairies, M., Mauduit, S., Michon, C., 2014. Rheological properties of starch suspensions using a rotational rheometer fitted with a starch stirrer cell. Rheol. Acta 53, 255–267.

Meeker, S.P., Bonnecaze, R.T., Cloitre, M., 2004. Slip and flow in pastes of soft particles: Direct observation and rheology. J. Rheol. 48, 1295–1320.

Mohammed, A.S., 2017. Effect of temperature on the rheological properties with shear stress limit of iron oxide nanoparticle modified bentonite drilling muds. Egyp. J. Pet. 26, 791–802.

Neaman, A., Singer, A., 2000. Rheology of mixed palygorskite-montmorillonite suspensions. Clays Clay Miner. 48, 713–715.

Nguyen, V.B.Q., Kang, H.S., Kim, Y.T., 2018. Effect of clay fraction and water content on rheological properties of sand-clay mixtures. Environ. Earth Sci. 77, 576.

O'Brien, J.S., Julien, P.Y., 1988. Laboratory analysis of mudflow properties. J. Hydraul. Eng. 114, 877–887.

Ovarlez, G., Cohen-Addad, S., Krishan, K., Goyon, J., Coussot, P., 2013. On the existence of a simple yield stress fluid behavior. J. Fluid NonNewton. Fluid Mech. 193, 68–79.

Ovarlez, G., Mahaut, F., Deboeuf, S., Lenoir, N., Hormozi, S., Chateau, X., 2015. Flows of suspensions of particles in yield stress fluids. J. Rheol. 59, 1449–1486.

Ovarlez, G., Rodts, S., Chateau, X., Coussot, P., 2009. Phenomenology and physical origin of shear localization and shear banding in complex fluids. Rheol. Acta 48, 831–844.

Pantet, A., Robert, S., Jarny, S., Kervella, S., 2010. Effect of coarse particle volume fraction on the yield stress of muddy sediments from Marennes Oléron Bay. Adv. Mater. Sci. Eng. 2010, 245398.

Paumier, S., 2007. Facteurs déterminant l'organisation et la rhéologie du système argile-eau pour des suspensions de smectites. University of Poitiers (France) PhD thesis.

Pellegrino, A.M., Schippa, L., 2018. A laboratory experience on the effect of grains concentration and coarse sediment on the rheology of natural debris-flows. Environ. Earth Sci. 77, 749.

Schall, P., Van Hecke, M., 2010. Shear bands in matter with granularity. Ann. Rev. Fluid Mech. 42, 67–88.

Shakeel, A., Kirichek, A., Chassagne, C., 2021a. Rheology and yielding transitions in mixed kaolinite/bentonite suspensions. Appl. Clay Sci. 211, 106206.

Shakeel, A., Kirichek, A., Talmon, A., Chassagne, C., 2021b. Rheological analysis and rheological modelling of mud sediments: What is the best protocol for maintenance of ports and waterways? Estuar. Coast. Shelf Sci. 257, 107407.

Spearman, J., 2017. An examination of the rheology of flocculated clay suspensions. Ocean Dyn. 6, 485–497.

Vipulanandan, C., Mohammed, A.S., 2014. Hyperbolic rheological model with shear stress limit for acrylamide polymer modified bentonite drilling muds. J. Pet. Sci. Eng. 122, 38–47.

Vu, T.S., Ovarlez, G., Chateau, X., 2018. Macroscopic behaviour of bidisperse suspensions of noncolloidal particles in yield stress fluids. J. Rheol. 54, 815–833.

Zhou, Z., Solomon, M.J., Scales, P.J., Boger, D.V., 1999. The yield stress of concentrated flocculated suspensions of size distributed particles. J. Rheol. 43, 651–671.